Understanding deep earth dynamics: a numerical modelling approach

Srishti Singh, Shubham Agrawal and Attreyee Ghosh*

Centre for Earth Sciences, Indian Institute of Science, Bengaluru 560 012, India

Enhancement in computing power and better data availability have paved the way for deciphering the earth's deeper dynamics and have provided viable explanations for various surface phenomena. Tools such as seismic tomography, numerical modelling and geophysical observations such as stresses, gravity anomalies, heat flow, etc. have helped us in addressing the mechanisms of plate driving forces, anomalous geoid variations, cratonic stability, topographic support, intraplate earthquakes and similar outstanding issues in geodynamics. Due to lack of direct observations from deep earth, numerical modelling has aided considerably in learning about subsurface processes. With better algorithms being developed everyday, it is the right time to tap their potential to push the frontiers of human knowledge.

Keywords: Geodynamics, lithosphere dynamics, mantle convection, numerical modelling, seismic tomography.

Introduction

IN the past 10,000 years, the time-span when modern humans have inhabited and dominated the earth, we have made steady progress to understand the planet we live in. Utilizing the strong foundations laid by scientists like Hutton, Wegener, Wilson and Rayleigh, amongst many others, earth sciences has progressed expeditiously in the last century. Research advancements in seismology, seafloor spreading, ocean bathymetry and geomagnetism paved the way for the most ground-breaking discovery in the field of earth sciences, the theory of plate tectonics. This century could see extraordinary progress in understanding subsurface dynamics of the earth, owing to the ongoing developments in computing.

The fundamental concern of geophysicists is to unravel the underlying physics behind the earth's processes. The earth is much more dynamically active than other planets (in the solar system), in terms of ongoing plate tectonics, convecting mantle, magnetically unstable core and vibrant atmosphere, thus providing a unique hospitable environment to sustain life. Earth is also rife with heterogeneities and complexities. Thus, understanding the earth and its processes is more intriguing and challenging. Significant technological advancements in the field of supercomputing and better algorithms to process the data have opened up new doors for geophysicists. Research in seismology, mantle and core dynamics, and mineral physics has benefited greatly from it.

The field of geodynamics deals with processes associated with the lithosphere and the mantle, and how these processes interact to result in surface expressions such as volcanism, mountain-building, earthquakes, rifting of continents, plate motions, gravity anomalies, etc. However, to study and understand these subsurface processes, we have to resort to indirect methods. Seismic tomography is the most popular and reliable method, which uses seismic data generated from earthquakes. Seismic tomography depicts the lateral deviation of velocity (δV) from a 1D reference velocity model such as preliminary reference earth model (PREM)[1]. Lower than average velocity could be the result of lower density material, and higher than average velocity could be due to higher density material[2]. Seismic tomography has been successful in tracing subducting slabs[3–6], upwelling plumes[7], cratons[3,8–10], large low shear velocity provinces (LLSVPs)[10–12], and several anomalous zones in the earth's interior.

Due to uncertainties and limited knowledge about deeper earth, numerical modelling proves to be a powerful tool to understand its dynamics. Lately, high-performance computing is widely used to study mantle convection and lithosphere dynamics, and how they relate to surface observations. The current research in computational geodynamics addresses many interesting questions about the earth. Some of these are: How does viscosity vary inside the earth and what role does it play in affecting convective flow within the mantle? How is strain accumulated and released at the plate boundaries? What is the mechanism of intraplate earthquakes? How have cratons survived for billions of years? How are mountains formed and supported? What gives rise to geoid anomalies? How do mantle and lithosphere couple to explain surface processes and what are their relative contributions? Here we give a brief overview of some of the aforementioned questions that we address using numerical modelling, tomography and other geophysical parameters.

*For correspondence. (e-mail: aghosh@ceas.iisc.ernet.in)

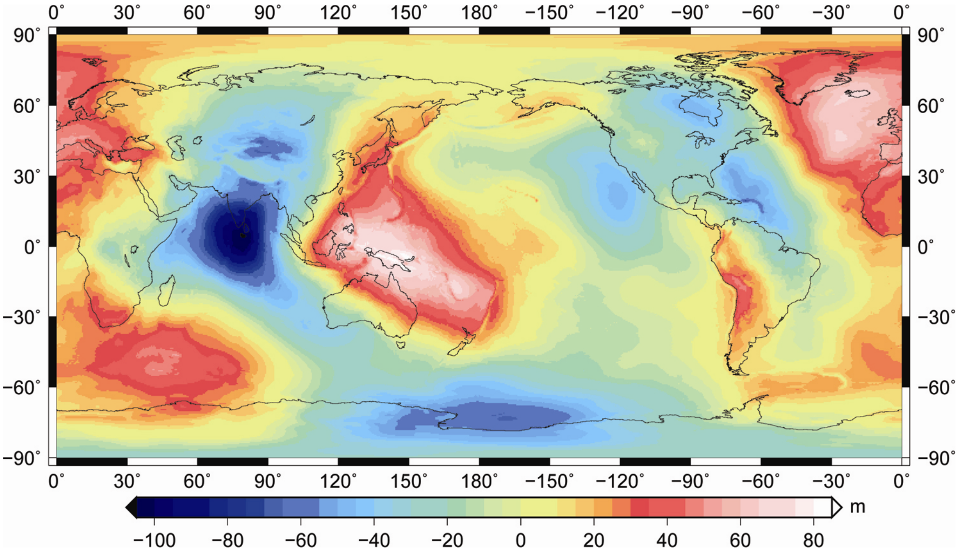

Figure 1. Global geoid from EGM-2008 model[137].

Geoid anomalies

Geoid is defined as a surface of equal gravitational potential which coincides with the mean sea level, and it is always perpendicular to the direction of gravity. Geoid anomalies result due to the variation of geoid surface from the reference ellipsoid. Geoid is best used to infer mass distribution within the earth's mantle[13,14] and is preferred over gravity as it is more sensitive to deeper sources.

The global geoid undulations are obtained with the help of satellites. Further, the geoid could be predicted through mantle convection modelling that takes into account seismic tomography models and history of past subductions along with radial viscosity variations (RVVs) and lateral viscosity variations (LVVs). The effects of RVVs on geoid are well studied by Richards and Hager[13]. They concluded that there is an increase in the earth's viscosity from upper to lower mantle. However, the effects of LVVs on geoid are still under debate[15–19].

The observed geoid has several anomalous zones in the form of highs and lows (Figure 1). The long-wavelength geoid highs are attributed to the presence of Pacific and African superplumes, while the short wavelength highs are well explained by subducting slabs[13]. The major regions of the geoid low are the Indian Ocean, Ross Sea, northeast Pacific Ocean and west Atlantic Ocean. Most of these geoid lows are ascribed to Mesozoic (250–70 Ma) subducted slabs[20]. However, geodynamic models have failed to replicate the geoid lows by incorporating lower mantle slabs from seismic tomography or from plate reconstruction history. Spasojevic *et al.*[21] revealed that geoid lows are associated with slow and fast seismic velocities in the upper and lower mantle respectively. The Indian Ocean Geoid Low (IOGL), south of the Indian subcontinent is regarded as the lowest geoid anomaly on earth with a value of –106 m south of Sri Lanka[22]. Negi *et al.*[23] proposed that such lows are caused by undulations on the core–mantle boundary (CMB) in agreement with the hypothesis that undulations on CMB cause long-wavelength geo-potential anomalies[24,25]. Rajesh[26], on the other hand, attributed IOGL to the presence of major density voids at depths of ~1800 km. Another study[27] proposed that IOGL results due to the accretion of low-density subducted Indian/Tethyan lithosphere at ~660 km discontinuity. A recent study[28] found seismic evidence for dehydrated slab graveyards above CMB beneath the Indian ocean, and linked it to IOGL. So the source of IOGL is still an open question and requires more studies in order to provide a definitive answer.

What supports topography?

It has been established that most of the surface topography has been created by thickening or thinning of the crust/lithosphere, which is a result of plate tectonics; but what has sustained these topographies over geological times? Airy[29] and Pratt[30] put forward the idea of isostasy as the major contender for supporting topography. Since then there has been significant technological advancement in understanding the nature of mantle convection and seismic tomography, leading to various long-wavelength topographies being attributed to the radial component of mantle flow, termed as dynamic topography[31,32]. The viscous stresses generated from interaction of mantle flow with surface boundary are balanced by gravitational stresses arising from vertical deflection of the surface[33]. The surface deflects upward in case of diverging flow (e.g. ridges) leading to positive dynamic topography,

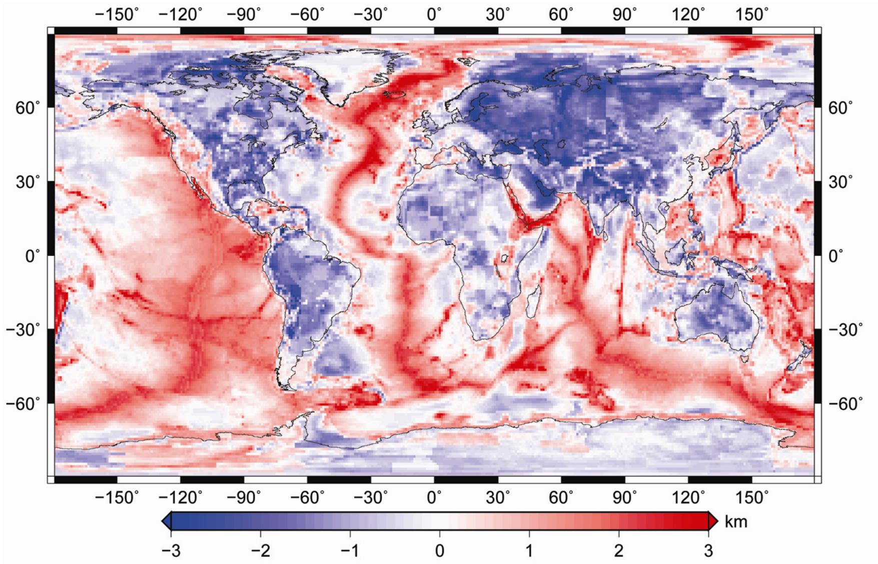

Figure 2. Residual topography obtained using crustal thickness from CRUST1.0 (ref. 138) and topography/bathymetry data from ETOPO1 (ref. 139) models.

while it deflects downward when the flow is convergent (e.g. subduction zones), resulting in negative dynamic topography. The amplitude of dynamic topography is directly proportional to the intensity and depth of mantle flow. The wavelength (or spatial extent) of dynamic topography is determined by the scale and depth of the mantle flow. As dynamic topography is usually transient in nature and has a low amplitude, it is hard to separate it from the isostatic part of topography. One way of distinguishing between isostatic and dynamic support is by using geoid-to-topography ratio (GTR)[34,35]. The amplitude of dynamic topography is estimated by subtracting the isostatically compensated topography from the total topography. The resultant topography is also known as residual topography[36,37] (Figure 2). Various studies predicted global dynamic topography as well using mantle flow models[38–41]. However, mantle flow models overestimate the amplitude of dynamic topography. The third type of support comes from the bending of the lithospheric plate known as flexure[42,43]. This support is purely elastic as opposed to isostatic and dynamic support.

Free-air gravity anomalies were shown to be good indicators of dynamically supported topography. However, Molnar *et al.*[44] argued that very small free-air gravity anomalies (<30 mGal) are associated with long-wavelength topographies, and most of them can be explained by isostatic equilibrium. To answer the apparent paradox, a recent study[45] showed that even without significant free air gravity anomaly, there could exist sizable dynamic topography using self-gravitating, viscously stratified earth models.

Over geological timescales, rocks behave as viscous material and have a tendency to flow. Hence topographically high regions tend to flatten out with time. However, regions with high elevation like the Tibetan plateau have sustained for a long period of time. So the question arises: what could have supported these topographies for such a long time? Horizontal mantle flow provides an effective mechanism for supporting these high topography regions[46].

Stability of cratons

Cratons are the stable parts of continents, where deformation has ceased at least from 750 Ma (Precambrian)[47]. From seismic and xenolith studies, it has been found that the cratons generally have thick roots of more than 200 km (Figure 3)[48–50]. Additionally, they are characterized by high seismic velocity[48] and low heat flux[51]. However, Singh and Negi[52] estimated high Moho temperatures in the Indian shield region and argued that this behaviour may be related to Deccan Trap volcanism and Himalayan orogeny.

Stability of the cratons is a unique problem in geophysics as it contradicts the concept of crustal recycling by mantle convection. Moreover, most of the cratons became stable during Archean (2500–3750 Ma)[53,54], when mantle heat flux was higher to support more vigorous convection[55]. There could be two end-member solutions to this problem[56]: (a) either cratons could resist deformation, or (b) they were avoided by the deforming agent (like mantle convection). Initial proposition was given by Jordan[57,58] that the cratonic mantle is compositionally buoyant, which gave it additional stability. Later, Lenardic and Moresi[56] showed that only buoyancy cannot provide the stability; rather it requires a strong material to resist deformation. Lenardic *et al.*[59] further demonstrated in their

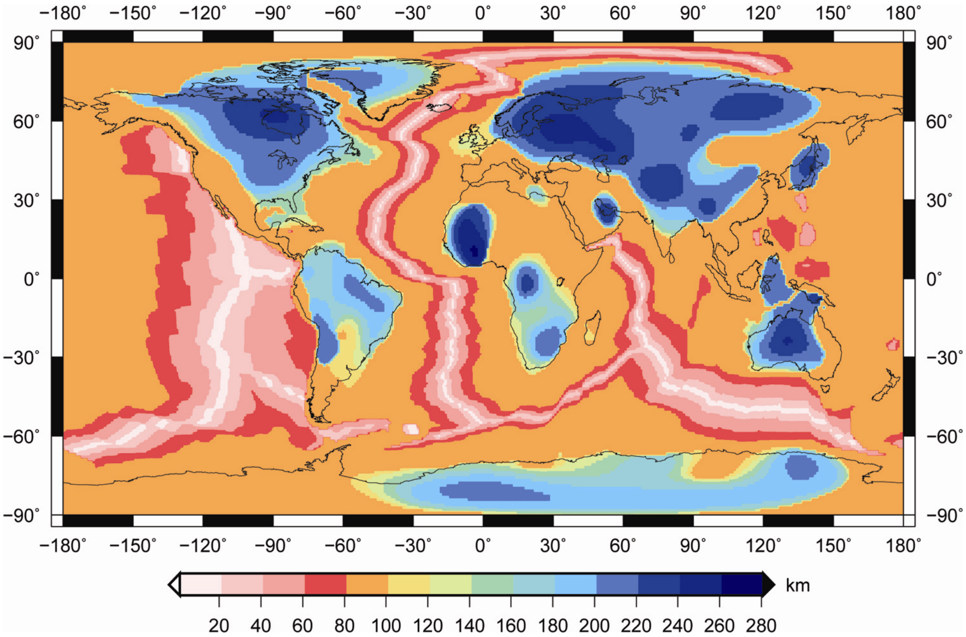

Figure 3. Global map of lithospheric thickness[140]. Blue regions corresponding to higher thickness are due to stable continental cratonic roots. Newly formed mid-oceanic ridges observed as white regions have the least lithospheric thickness on earth.

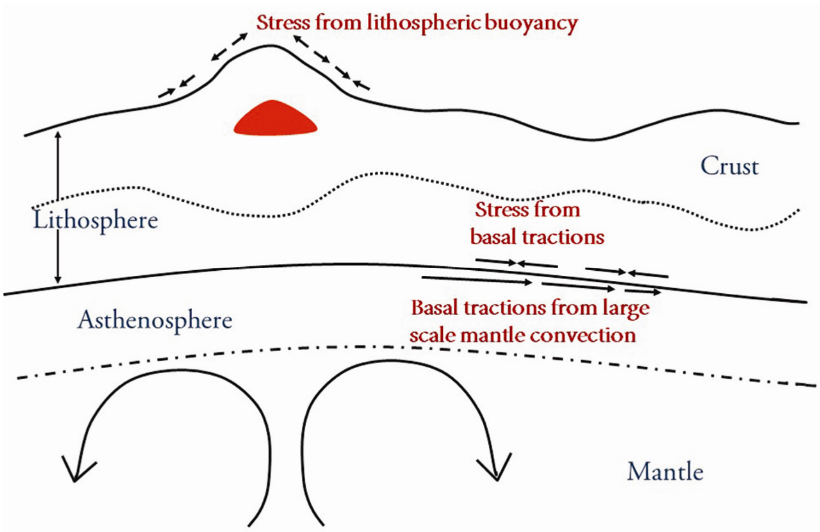

Figure 4. Schematic showing how lithosphere dynamics and mantle convection contribute to the forces driving plate tectonics.

numerical modelling studies that cratonic stability could be obtained by applying suitable viscosity, thickness, yield strength and surrounding weak zones.

The problem of cratonic stability is being addressed during the last 40 years either by theoretical or numerical approach, but a realistic 3D earth-like model is yet to be developed. Models proposed by Lenardic *et al.*[59], have shown cratonic stability till 175 Ma, which is quite a short period of time compared to earth's history. Yoshida[60] numerically showed the stability of cratonic blocks till 2000 Ma, by using a very high viscosity contrast between the craton and surrounding materials. However, validation of this assumption is yet to be confirmed.

Furthermore, the thickness of the cratonic lithosphere has been difficult to constrain by seismic tomography and receiver function studies as lithosphere–asthenosphere boundary is not sharply defined at many places. Recent studies have suggested a thickness of 200–250 km by incorporating the effects of anisotropy on seismic velocities[61]. However, at shallower depths (100–140 km) beneath these cratons, strong conversions from compressional-to-shear wave (*P–S*) and shear-to-compressional wave (*S–P*) have been found[62–64]. This led some researchers to believe that the thickness of the cratonic lithosphere might be less than expected[62], which contradicts tomographic and other geophysical and geochemical

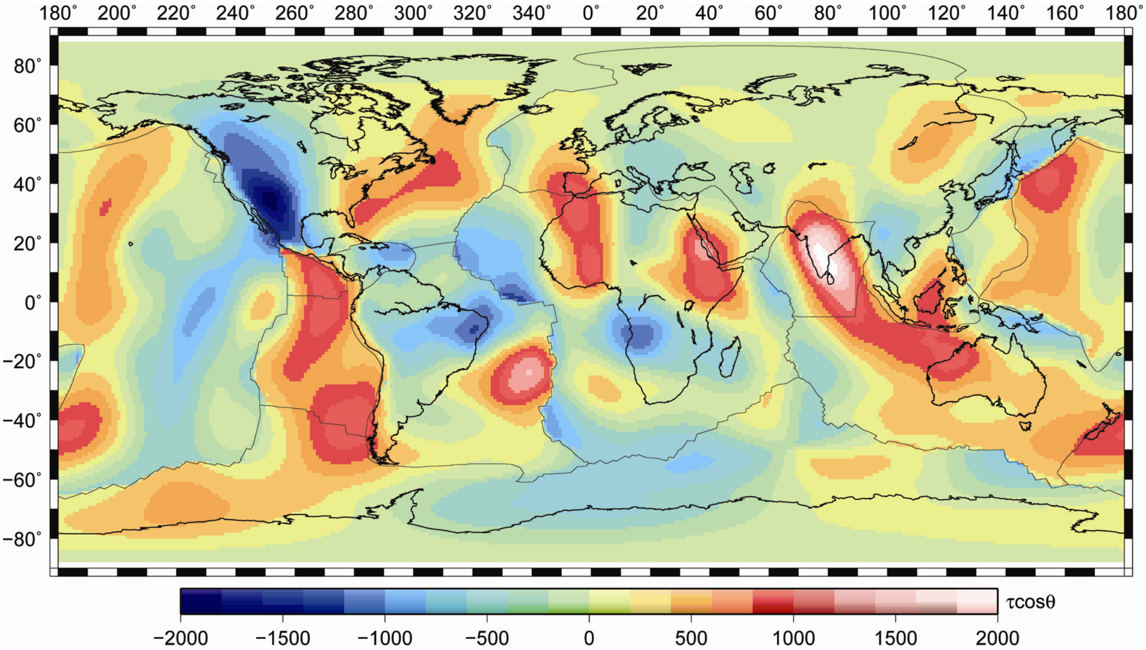

Figure 5. Quantitative measure of whether mantle tractions are driving or resisting plate motions. Blue regions (negative values) show resisting tractions while red regions (positive) denote that tractions are the main drivers (source: Ghosh *et al.*[69]).

observations. Therefore, such conversions have been recently attributed to the presence of an intracontinental discontinuous zone of either partial melt or dehydrated material, or both, around depths of 100 km (ref. 65), known as mid-lithospheric boundary (MLB)[66]. However, the presence of MLB on a global scale is still a controversial topic.

Forces driving plate tectonics

The forces that drive plate tectonics and cause deformations which lead to mountain-building, rifting of continents, volcanism, etc. are not well established. Geodynamic modelling takes into account two main forces driving plate tectonics: the first is due to gravitational potential energy (GPE) variations, and the second results from long-wavelength tractions produced by density-driven flow in the mantle.

In addition to varying crustal thickness and topography, GPE variations also arise due to lateral density variations within the lithosphere. In simple terms, high GPE area has high-density material or high topography, or both. Similarly, a low GPE will reflect the presence of low-density material or low topography. GPE gradients give rise to deviatoric stresses which cause deformation. The long-wavelength flow driven by density anomalies within the mantle generates tractions that act at the base of the lithosphere, also producing deviatoric stresses (Figure 4). These tractions are modelled via fluid dynamical models of convecting mantle flow driven by density variations as inferred from tomography and subduction plate history (cf. refs 67, 68).

A major question till date is how do mantle tractions couple with the lithosphere and to what extent? Few studies have tried to address this question by modelling both sources[69–74]. These studies showed that coupling depends on the viscosity variations. A low-viscosity asthenosphere would decouple the mantle from the lithosphere, while a highly viscous one would enhance the coupling. Another interesting and controversial question is: do mantle tractions assist or resist plate motion? Ghosh *et al.*[69] argued that in areas like the Nazca plate, eastern North America, North Atlantic, Indo-Australian plate, etc. mantle flow is driving plate motion. On the other hand, in places like western North America, the northern part of South America and southern Africa, tractions are resistive, and so plates are driving the mantle flow (Figure 5).

Intra-plate earthquakes

With the advent of GPS data, we are able to measure plate movement and deformation more accurately. Although we are still not able to predict earthquakes, but we can make realistic forecasts. If an active fault zone is locked and GPS data suggest strain build-up, the region might be storing up energy to be released in the form of earthquakes[76,77]. Large devastating earthquakes like Sumatra (2004), Haiti (2010), Tohuku (2011) and Nepal (2015) made us realize that accurate forecasting of earthquakes is extremely important.

Typically, earthquakes occur at plate boundaries which are continuously deforming, but what about those that happen in the interior of continents, away from the plate

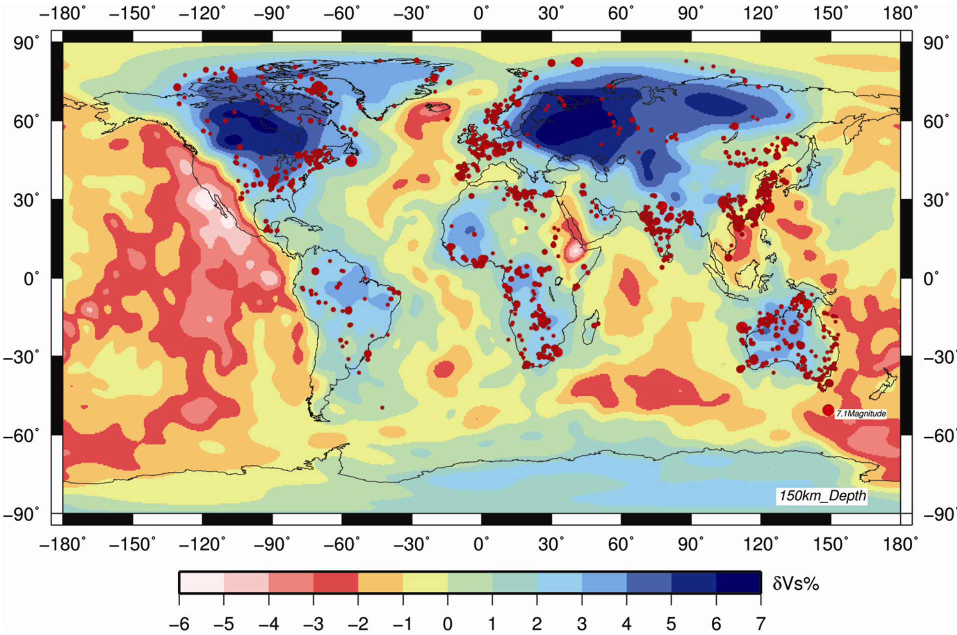

Figure 6. Stable continental regions seismicity catalogue obtained from Schulte and Mooney[75] (red circles), plotted on a global map of shear wave velocity perturbations (S40RTS model)[10] at a depth of 150 km.

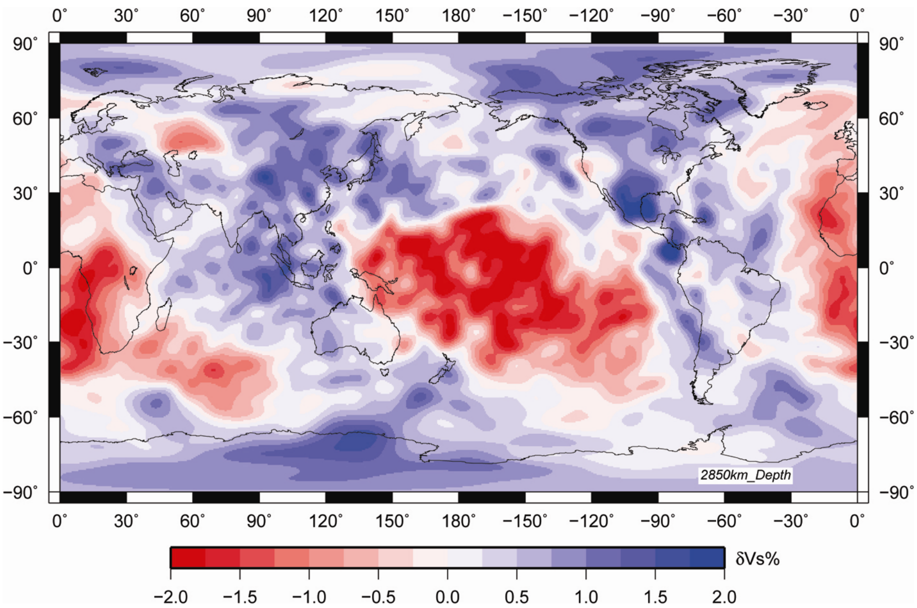

Figure 7. Plot of S-wave velocity anomalies at a depth of 2850 km (near CMB) using the S40RTS model[10]. LLSVPs are shown by two large antipodal red regions of negative δV_s.

boundaries? These types of earthquakes are generally referred to as intraplate earthquakes (IPEs). A major subset of IPEs occurs in stable continental regions (SCRs) (Figure 6)[78]. The most widely accepted theory of plate tectonics is unable to explain the occurrence of IPEs. One might argue that IPEs occur on palaeo-faults or weak zones, which were once part of active tectonics. Studies have repeatedly reported significantly low geodetic strain rates in SCRs like New Madrid Seismic Zone (NMSZ) (0.2 mm/yr) (refs 79, 80), Europe (0.2 mm/yr) (ref. 81), South Africa (0.6 mm/yr) (ref. 82) and Australia (0.2 mm/yr) (ref. 83), which are all seismically active. These values are almost indistinguishable from zero and no other seismically active SCRs have been identified with measurable strain rates[84]. So without any significant strain rate, how are earthquakes materializing in these defunct faults?

Although of lower magnitude than plate boundary earthquakes, IPEs could be more calamitous because they impact areas that are not accustomed to earthquakes and where buildings are not usually seismically retrofitted. For example, the 2001 Bhuj, India earthquake (M_w 7.7) claimed about 20,000 lives[85,86]. Even the 1993 Latur earthquake, which was of moderate magnitude (M_w 6.2), claimed thousands of lives[87]. Therefore, there have been several attempts to understand IPEs and their probable causes. Studies have been carried out to find a correlation between intraplate seismicity and some other physical parameter. It had been proposed that higher heat flow values might weaken the crust and thus make SCRs prone to seismicity[88]. Regional studies in NMSZ[89] (site of the three famous 1811–12 $M_w \geqslant 7$ earthquakes, and continued seismicity of $M_w < 5$ till now), western Europe and southern Australia[90], all tell different stories. Thus, no clear correlation has been established between heat flow and IPEs. A different, widely accepted notion is that IPEs tend to happen more in ancient rift margins. Schulte and Mooney[75] presented the updated SCR earthquake catalogue and assessed the correlation of IPEs with ancient rifts on a global scale and found that it has been overestimated in the past (36% occurred in non-rifted crust). Other models have suggested that seismicity in continental interiors could be due to intersecting faults[91], crustal anomalies[92,93], etc. Mooney *et al.*[94] used *S*-wave seismic velocity anomaly[10] to find a correlation with SCR seismicity. They found that for the North American continent, stable continental cratons ($\delta V_s \geqslant 3$) are least prone to seismicity, while there is a clearly visible increased seismicity at the edge of these cratons. However, our recent work has suggested that correlation with craton edge is strong for North America, but weak for other continents. To further scrutinize the correlation, we have used a recent tomography model (SEMUCB-WM1)[95] and found that seismicity patterns are different for each continent. Also, Australia showed a stark contrast to the results of Mooney *et al.*[94]. However, this is an ongoing research and more work is required to draw a definitive conclusion.

Another major issue regarding IPEs is how stress builds up in these areas. Models have used lateral viscosity variations[94] and crustal density variations[96] to explain seismicity. Lately, geophysical parameters like gravitational potential energy, dynamic topography, large-scale tectonic forces, and glacial isostatic adjustment (GIA) have also been used to explain the occurrence of IPEs[97,98]. Therefore, there is no consensus on explaining IPEs and they remain an exciting topic of research.

Large low shear velocity provinces

Mantle convection has two major components: rising plumes and downwelling slabs. The origin of downwelling slabs lies in subduction zones while the origin of plumes is a topic of active research. Some researchers believe that hotspots (intraplate volcanism) have a shallow source[99,100], while others argue that their sources are deeper, originating from the margins of LLSVPs[101–103]. LLSVPs are massive anomalous zones with velocity deviations of $\delta V_s < -1\%$ near CMB[104,105]. Tomography has been used extensively to study them and many tomography models[10,95,106–108] have captured two LLSVPs, one under the Pacific Ocean and the other beneath the African continent (Figure 7).

The LLSVP under the Pacific is more or less elliptical, but the shape of the LLSVP under Africa is rather elongated. The overall shape and size of these low-velocity zones differ from model to model, with differences in short scales[105,109]. It has been modelled and hypothesized that LLSVPs have different thermal and chemical properties than the surrounding mantle[110–112]; thus these are also termed as ‘thermochemical piles’. LLSVPs are stable for a longer period of time and are considered to have a higher density than the surrounding mantle[113,114].

Two theories have been proposed to explain their genesis: they have been accreting continuously from the beginning of the earth[115,116], or an already present layer (formed from differentiation process during early earth) gradually shaped into the current LLSVPs[117–119]. The stability of these structures depends on the amount and rate at which material is being added and lost in the form of subducted slabs and plumes respectively, which is currently unknown.

Plumes have been traced recently using tomography[7]. These plumes rising from the margin of the LLSVPs have been linked to large igneous provinces (LIPs), hotspots (e.g. Hawaii, Reunion, Yellowstone), and kimberlites (South Africa)[101–103,120]. These hotspots often result in the formation of LIPs (e.g. Siberian trap and Deccan trap) as a result of intense volcanism. All hotspots and almost 80% of the LIP sources have been linked to the margin of the LLSVPs, thus bolstering the theory that hotspots and LIPs have deep mantle sources, as opposed to shallow sources. Moreover, numerical models have confirmed the feasibility of plumes from the CMB[103,121]. However, it is still unclear how these plumes interact with the overlying lithosphere[122].

A logical question that comes to mind is how do these low-velocity (low-density?) zones have density variations such that they are stable and reside at the CMB? Even though the assumption is that velocity is proportional to density, the relation is subject to temperature, pressure and chemical composition. The chemical properties of material change a lot under intense pressure as we go deeper into the earth. Although the existence of LLSVPs is well established, there exist several unanswered questions regarding them.

Discussion

The last few decades have seen a lot of progress in understanding the deeper dynamics of the earth. Although seismic tomography has proved to be a useful tool to infer about subsurface lateral density distribution[3,123–125], it has always been a major concern to relate seismic velocity to density perturbations. Generally, a velocity–density scaling ($R_{\rho/s} = d\ln\rho/d\ln V_s$) is used to convert seismic velocities to densities based on mineral physics experiments. The scaling is still not well constrained throughout the mantle and is based on the assumption that density perturbations are purely thermal in origin[126,127]. However, this assumption does not hold for portions of the upper mantle beneath compositionally distinct cratons[58,128] and the lower mantle close to the CMB, as revealed by various studies[123,124,129–131]. Another prominent evidence against the solely thermal origin of mantle heterogeneities comes from significant variations observed in bulk sound and shear wave velocities in deep mantle[123,130,132,133]. In deep mantle, the correlation between seismic velocity anomalies and density perturbations was found to be weaker at some places, and even anti-correlated in some regions, the indicating presence of compositional heterogeneities[123,131–133]. Thus an important question is whether compositional variations play a major role in affecting overall mantle convection[108], which is still unanswered.

Another major debate in the geophysical community has been about the existence of plumes, as they are not integral to the theory of plate tectonics. As opposed to subducting slabs, mantle plumes were not detected in seismic tomographic images. Only very recently, French and Romanowicz[7] traced vertical low velocity anomalies beneath several hotspots up to a depth of 1000 km, thus supporting the deep origin of hotspot magma. Another school of thought believes that hotspots have much shallower magma sources similar to mid-oceanic ridges, which are driven by shear processes in the top layer (plate tectonics) and not by deep upwellings[99,100].

Although density variations are the main drivers of mantle convection, viscosity also plays an important role. Our knowledge about viscosity structure of mantle is quite limited. A major hindrance to model mantle flow is the unavailability of realistic viscosity profiles. Radial viscosity distribution can be inferred indirectly from geophysical observations such as geoid[134] and GIA studies[135,136]. However, the effect of lateral viscosity variations on mantle convection is still not well established[17–19].

Increase in computing power and better quality of data have given geoscientists a new tool to access the mysteries of the earth. For example, the recent US Array experiment, that explores the lithosphere and upper mantle structure beneath North America using seismic waves, is giving us an unprecedented view of many subsurface structures and mechanisms. Be it imaging the pathways of fluids and magma within the earth, understanding the earth's deformation, or looking into deep earth's structure, current research in geodynamics is giving us more clues about how this planet works. We have made steady progress to achieve our aim to comprehend our planet, but we still have a long way to go.

1. Dziewonski, A. M. and Anderson, D. L., Preliminary reference Earth model. *Phys. Earth Planet. Inter.*, 1981, **25**(4), 297–356.
2. Karato, S., Importance of anelasticity in the interpretation of seismic tomography. *Geophys. Res. Lett.*, 1993, **20**(15), 1623–1626.
3. Grand, S. P., van der Hilst, R. D. and Widiyantoro, S., High resolution global tomography: a snapshot of convection in the Earth. *Geol. Soc. Am. Today*, 1997, **7**(4), 1–7.
4. Fukao, Y., Widiyantoro, S. and Obayashi, M., Stagnant slabs in the upper and lower mantle transition region. *Rev. Geophys.*, 2001, **39**(3), 291–323.
5. Zhao, D., Global tomographic images of mantle plumes and subducting slabs: insight into deep Earth dynamics. *Phys. Earth Planet. Inter.*, 2004, **146**(12), 3–34.
6. Simmons, N. A., Myers, S. C., Johannesson, G., Matzel, E. and Grand, S. P., Evidence for long-lived subduction of an ancient tectonic plate beneath the southern Indian Ocean. *Geophys. Res. Lett.*, 2015, **42**(21), 9270–9278.
7. French, S. W. and Romanowicz, B., Broad plumes rooted at the base of the Earth's mantle beneath major hotspots. *Nature*, 2015, **525**(7567), 95–99.
8. Woodhouse, J. H. and Dziewonski, A. M., Mapping the upper mantle: three-dimensional modeling of earth structure by inversion of seismic waveforms. *J. Geophys. Res. B*, 1984, **89**(7), 5953–5986.
9. Romanowicz, B., The thickness of tectonic plates. *Science*, 2009, **324**(5926), 474–476.
10. Ritsema, J., Deuss, A., van Heijst, H. J. and Woodhouse, J. H., S40RTS: a degree-40 shear-velocity model for the mantle from new Rayleigh wave dispersion, teleseismic traveltime and normal-mode splitting function measurements. *Geophys. J. Inter.*, 2011, **184**(3), 1223–1236.
11. Dziewonski, A. M., Mapping the lower mantle: determination of lateral heterogeneity in *P* velocity up to degree and order 6. *J. Geophys. Res. B*, 1984, **89**(7), 5929–5952.
12. Burke, K., Steinberger, B., Torsvik, T. H. and Smethurst, M. A., Plume generation zones at the margins of large low shear velocity provinces on the core–mantle boundary. *Earth Planet. Sci. Lett.*, 2008, **265**(1), 49–60.
13. Richards, M. A. and Hager, B. H., Geoid anomalies in a dynamic Earth. *J. Geophys. Res. B*, 1984, **89**(7), 5987–6002.
14. Forte, A. M. and Mitrovica, J. X., Deep-mantle high-viscosity flow and thermochemical structure inferred from seismic and geodynamic data. *Nature*, 2001, **410**(6832), 1049–1056.
15. King, S. D. and Hager, B. H., Sub-ducted slabs and the geoid: 1. Numerical experiments with temperature-dependent viscosity. *J. Geophys. Res. B*, 1994, **99**(10), 19843–19852.
16. Čadek, O. and Fleitout, L., Effect of lateral viscosity variations in the top 300 km on the geoid and dynamic topography. *Geophys. J. Int.*, 2003, **152**(3), 566–580.
17. Zhong, S. and Davies, G. F., Effects of plate and slab viscosities on the geoid. *Earth Planet. Sci. Lett.*, 1999, **170**(4), 487–496.
18. Moucha, R., Forte, A., Mitrovica, J. and Daradich, A., Lateral variations in mantle rheology: implications for convection related surface observables and inferred viscosity models. *Geophys. J. Int.*, 2007, **169**(1), 113–135.
19. Ghosh, A., Becker, T. and Zhong, S., Effects of lateral viscosity variations on the geoid. *Geophys. Res. Lett.*, 2010, **37**(1), L01301; doi:10.1029/2009GL040426.
20. Chase, C. G. and Sprowl, D. R., The modern geoid and ancient plate boundaries. *Earth Planet. Sci. Lett.*, 1983, **62**(3), 314–320.

21. Spasojevic, S., Gurnis, M. and Sutherland, R., Mantle upwellings above slab graveyards linked to the global geoid lows. *Nature Geosci.*, 2010, **3**(6), 435–438.
22. Sreejith, K., Rajesh, S., Majumdar, T., Rao, G. S., Radhakrishna, M., Krishna, K. and Rajawat, A., High-resolution residual geoid and gravity anomaly data of the northern Indian Ocean – an input to geological understanding. *J. Asian Earth Sci.*, 2013, **62**, 616–626.
23. Negi, J., Thakur, N. and Agrawal, P., Can depression of the core-mantle interface cause coincident Magsat and geoidal lows of the Central Indian Ocean? *Phys. Earth Planet. Inter.*, 1987, **45**(1), 68–74.
24. Hide, R., Interaction between the Earth's liquid core and solid mantle. *Nature*, 1969, **222**, 1055–1056.
25. Hide, R. and Malin, S., Novel correlations between global features of the earth's gravitational and magnetic fields. *Nature*, 1970, **230**(11), 63.
26. Rajesh, S., Geoid and the regional density anomaly field in the Indian Plate. *Himalayan Geol.*, 2009, **30**(2), 187–192.
27. Mishra, D., Kumar, M. R. and Arora, K., Long wavelength satellite gravity and geoid anomalies over Himalaya and Tibet: lithospheric structures and seismotectonics of deep focus earthquakes of Hindu Kush–Pamir and Burmese arc. *J. Asian Earth Sci.*, 2012, **48**, 93–110.
28. Rao, B. P. and Kumar, M. R., Seismic evidence for slab graveyards atop the core–mantle boundary beneath the Indian Ocean geoid low. *Phys. Earth Planet. Inter.*, 2014, **236**, 52–59.
29. Airy, G. B., On the computation of the effect of the attraction of mountain-masses, as disturbing the apparent astronomical latitude of stations in geodetic surveys. *Philos. Trans. R. Soc. London*, 1855, **145**, 101–104.
30. Pratt, J. H., On the attraction of the Himalaya Mountains, and of the elevated regions beyond them, upon the plumb-line in India. *Philos. Trans. R. Soc. London*, 1855, **145**, 53–100.
31. Hager, B., Clayton, R., Richards, M., Comer, R. and Dziewonski, A., Lower mantle heterogeneity, dynamic topography and the geoid. *Nature*, 1985, **313**, 541–545.
32. Forte, A., Peltier, W., Dziewonski, A. and Woodward, R., Dynamic surface topography: a new interpretation based upon mantle flow models derived from seismic tomography. *Geophys. Res. Lett.*, 1993, **20**(3), 225–228.
33. Braun, J., The many surface expressions of mantle dynamics. *Nature Geosci.*, 2010, **3**(12), 825–833.
34. Sandwell, D. T. and MacKenzie, K. R., Geoid height versus topography for oceanic plateaus and swells. *J. Geophys. Res. B*, 1989, **94**(6), 7403–7418.
35. Coblentz, D., Chase, C., Karlstrom, K. and van Wijk, J., Topography, the geoid, and compensation mechanisms for the southern Rocky Mountains. *Geochem., Geophys., Geosyst.*, 2011, **12**, Q04002; doi:10.1029/2010GC003459.
36. Panasyuk, S. V. and Hager, B. H., Models of isostatic and dynamic topography, geoid anomalies, and their uncertainties. *J. Geophys. Res. Solid Earth*, 2000, **105**(B12), 28199–28209.
37. Wang, Y., Huang, J., Zhong, S. and Chen, J., Heat flux and topography constraints on thermochemical structure below North China Craton regions and implications for evolution of cratonic lithosphere. *J. Geophys. Res. B*, 2016, **121**(4), 3081–3098.
38. Boschi, L., Becker, T. and Steinberger, B., Mantle plumes: dynamic models and seismic images. *Geochem., Geophys., Geosyst.*, 2007, **8**, Q10006; doi:10.1029/2007GC001733.
39. Conrad, C. P. and Husson, L., Influence of dynamic topography on sea level and its rate of change. *Lithosphere*, 2009, **1**(2), 110–120.
40. Lithgow-Bertelloni, C. and Silver, P. G., Dynamic topography, plate driving forces and the African supers well. *Nature*, 1998, **395**(6699), 269–272.
41. Flament, N., Gurnis, M. and Müller, R. D., A review of observations and models of dynamic topography. *Lithosphere*, 2013, **5**(2), 189–210.
42. Forsyth, D. W., Subsurface loading and estimates of the flexural rigidity of continental lithosphere. *J. Geophys. Res. B*, 1985, **90**(14), 12623–12632.
43. McKenzie, D. and Fairhead, D., Estimates of the effective elastic thickness of the continental lithosphere from Bouguer and free air gravity anomalies. *J. Geophys. Res. B*, 1997, **102**(12), 27523–27552.
44. Molnar, P., England, P. C. and Jones, C. H., Mantle dynamics, isostasy, and the support of high terrain. *J. Geophys. Res. B*, 2015, **120**(3), 1932–1957.
45. Colli, L., Ghelichkhan, S. and Bunge, H.-P., On the ratio of dynamic topography and gravity anomalies in a dynamic Earth. *Geophys. Res. Lett.*, 2016, 2510–2516.
46. Ghosh, A., Holt, W. E., Flesch, L. M. and Haines, A. J., Gravitational potential energy of the Tibetan Plateau and the forces driving the Indian plate. *Geology*, 2006, **34**(5), 321–324.
47. King, S. D., Archean cratons and mantle dynamics. *Earth Planet. Sci. Lett.*, 2005, **234**(1), 1–14.
48. Polet, J. and Anderson, D. L., Depth extent of cratons as inferred from tomographic studies. *Geology*, 1995, **23**(3), 205–208.
49. Artemieva, I. M. and Mooney, W. D., On the relations between cratonic lithosphere thickness, plate motions, and basal drag. *Tectonophysics*, 2002, **358**(1), 211–231.
50. Coope, C. and Conrad, C. P., Does the mantle control the maximum thickness of cratons? *Lithosphere*, 2009, **1**(2), 67–72.
51. Rudnick, R. L., McDonough, W. F. and O'Connell, R. J., Thermal structure, thickness and composition of continental lithosphere. *Chem. Geol.*, 1998, **145**(3), 395–411.
52. Singh, R. N. and Negi, J. G., High Moho temperature in the Indian shield. *Tectonophysics*, 1982, **82**(3–4), 299–306.
53. Pearson, D., Carlson, R., Shirey, S., Boyd, F. and Nixon, P., Stabilisation of Archaean lithospheric mantle: a Re–Os isotope study of peridotite xenoliths from the Kaapvaal craton. *Earth Planet. Sci. Lett.*, 1995, **134**(3), 341–357.
54. Pearson, D., Snyder, G. and Shireyf, S., Archaean Re–Os age for Siberian eclogites and constraints on Archaean tectonics. *Nature*, 1995, **374**, 711–713.
55. Korenaga, J., Initiation and evolution of plate tectonics on Earth: theories and observations. *Annu. Rev. Earth Planet. Sci.*, 2013, **41**, 117–151.
56. Lenardic, A. and Moresi, L.-N., Some thoughts on the stability of cratonic lithosphere: effects of buoyancy and viscosity. *J. Geophys. Res. B*, 1999, **104**(6), 12747–12758.
57. Jordan, T. H., The continental tectosphere. *Rev. Geophys.*, 1975, **13**(3), 1–12.
58. Jordan, T. H., Composition and development of the continental tectosphere. *Nature*, 1978, **274**(5671), 544–548.
59. Lenardic, A., Moresi, L.-N. and Mühlhaus, H., Longevity and stability of cratonic lithosphere: insights from numerical simulations of coupled mantle convection and continental tectonics. *J. Geophys. Res. B*, 2003, **108**, 2303; doi:10.1029/2002JB001859.
60. Yoshida, M., Dynamic role of the rheological contrast between cratonic and oceanic lithospheres in the longevity of cratonic lithosphere: A three-dimensional numerical study. *Tectonophysics*, 2012, **532**, 156–166.
61. Gung, Y., Panning, M. and Romanowicz, B., Global anisotropy and the thickness of continents. *Nature*, 2003, **422**(6933), 707–711.
62. Rychert, C. A. and Shearer, P. M., A global view of the lithosphere–asthenosphere boundary. *Science*, 2009, **324**(5926), 495–498.
63. Abt, D. L., Fischer, K. M., French, S. W., Ford, H. A., Yuan, H. and Romanowicz, B., North American lithospheric discontinuity structure imaged by Ps and Sp receiver functions. *J. Geophys. Res. B*, 2010, **115**, B09301; doi:10.1029/2009JB006914..
64. Yuan, X., Kind, R., Li, X. and Wang, R., The *S* receiver functions: synthetics and data example. *Geophys. J. Int.*, 2006, **165**(2), 555–564.

65. Romanowicz, B., The thickness of tectonic plates. *Science*, 2009, **324**(5926), 474–476.
66. Yuan, H. and Romanowicz, B., Lithospheric layering in the North American craton. *Nature*, 2010, **466**(7310), 1063–1068.
67. Zhong, S., Yuen, D. A. and Moresi, L. N., Numerical methods for mantle convection. *Treatise Geophys.*, 2007, **7**, 227–252.
68. Wen, L. and Anderson, D. L., Layered mantle convection: a model for geoid and topography. *Earth Planet. Sci. Lett.*, 1997, **146**(3), 367–377.
69. Ghosh, A., Holt, W. and Wen, L., Predicting the lithospheric stress field and plate motions by joint modeling of lithosphere and mantle dynamics. *J. Geophys. Res. B*, 2013, **118**(1), 346–368.
70. Bird, P., Testing hypotheses on plate-driving mechanisms with global lithosphere models including topography, thermal structure, and faults. *J. Geophys. Res. B*, 1998, **103**(5), 10115–10129.
71. Bai, W., Vigny, C., Ricard, Y. and Froidevaux, C., On the origin of deviatoric stresses in the lithosphere. *J. Geophys. Res. B*, 1992, **97**(8), 11729–11737.
72. Steinberger, B., Schmeling, H. and Marquart, G., Large-scale lithospheric stress field and topography induced by global mantle circulation. *Earth Planet. Sci. Lett.*, 2001, **186**(1), 75–91.
73. Ghosh, A., Holt, W., Wen, L., Haines, A. and Flesch, L., Joint modeling of lithosphere and mantle dynamics elucidating lithosphere–mantle coupling. *Geophys. Res. Lett.*, 2008, **35**, L16309; doi:10.1029/2008GL034365.
74. Ghosh, A. and Holt, W., Plate motions and stresses from global dynamic models. *Science*, 2012, **335**(6070), 838–843.
75. Schulte, S. M. and Mooney, W. D., An updated global earthquake catalogue for stable continental regions: reassessing the correlation with ancient rifts. *Geophys. J. Int.*, 2005, **161**(3), 707–721.
76. Bollinger, L., Avouac, J. P., Cattin, R. and Pandey, M. R., Stress buildup in the Himalaya. *J. Geophys. Res. B*, 2004, **109**(B11405); doi:10.1029/2003JB002911.
77. Scholz, C. H., *The Mechanics of Earthquakes and Faulting*, Cambridge University Press, 2002.
78. Johnston, A. C., Coppersmith, K. J., Kanter, L. R. and Cornell, C. A., The earthquakes of stable continental regions. Tech. Rep. TR-102261, Electric Power Research Institute (EPRI), Palo Alto, CA, 1994.
79. Craig, T. J. and Calais, E., Strain accumulation in the New Madrid and Wabash Valley seismic zones from 14 years of continuous GPS observation. *J. Geophys. Res. B*, 2014, **119**(12), 9110–9129.
80. Boyd, O. S., Smalley, R. and Zeng, Y., Crustal deformation in the New Madrid seismic zone and the role of postseismic processes. *J. Geophys. Res. B*, 2015, **120**(8), 5782–5803.
81. Nocquet, J.-M., Present-day kinematics of the Mediterranean: a comprehensive overview of GPS results. *Tectonophysics*, 2012, **579**, 220–242.
82. Saria, E., Calais, E., Altamimi, Z., Willis, P. and Farah, H., A new velocity field for Africa from combined GPS and DORIS space geodetic solutions: Contribution to the definition of the African reference frame (AFREF). *J. Geophys. Res. B*, 2013, **118**(4), 1677–1697.
83. Tregoning, P., Burgette, R., McClusky, S., Lejeune, S., Watson, C. S. and McQueen, H., A decade of horizontal deformation from great earthquakes. *J. Geophys. Res. B*, 2013, **118**(5), 2371–2381.
84. Calais, E., Camelbeeck, T., Stein, S., Liu, M. and Craig, T. J., A new paradigm for large earthquakes in stable continental plate interiors. *Geophys. Res. Lett.*, 2016, **43**(20), 10621–10637.
85. Rajendran, K., Rajendran, C., Thakkar, M. and Tuttle, M. P., The 2001 Kutch (Bhuj) earthquake: coseismic surface features and their significance. *Curr. Sci.*, 2001, **80**(11), 1397–1405.
86. Gupta, H. K., Rao, N. P., Rastogi, B. and Sarkar, D., The deadliest intraplate earthquake. *Science*, 2001, **291**(5511), 2101–2102.
87. Gupta, H. K., The deadly Latur earthquake. *Science*, 1993, **262**(5140), 1666–1667.
88. Liu, L. and Zoback, M. D., Lithospheric strength and intraplate seismicity in the New Madrid seismic zone. *Tectonics*, 1997, **16**(4), 585–595.
89. McKenna, J., Stein, S. and Stein, C. A., Is the New Madrid seismic zone hotter and weaker than its surroundings? *Geol. Soc. Am. Spec. Pap.*, 2007, **425**, 167–175.
90. Holford, S., Hillis, R., Duddy, I., Green, P., Tassone, D. and Stoker, M., Paleothermal and seismic constraints on late Miocene–Pliocene uplift and deformation in the Torquay sub-basin, southern Australian margin. *Aust. J. Earth Sci.*, 2011, **58**(5), 543–562.
91. Talwani, P., Fault geometry and earthquakes in continental interiors. *Tectonophysics*, 1999, **305**(1), 371–379.
92. Campbell, D. L., Investigation of the stress concentration mechanism for intraplate earthquakes. *Geophys. Res. Lett.*, 1978, **5**(6), 477–479.
93. Kenner, S. J. and Segall, P., A mechanical model for intraplate earthquakes: application to the New Madrid seismic zone. *Science*, 2000, **289**(5488), 2329–2332.
94. Mooney, W. D., Ritsema, J. and Hwang, Y. K., Crustal seismicity and the earthquake catalog maximum moment magnitude (M cmax) in stable continental regions (SCRs): correlation with the seismic velocity of the lithosphere. *Earth Planet. Sci. Lett.*, 2012, **357**, 78–83.
95. French, S. and Romanowicz, B., Whole-mantle radially anisotropic shear velocity structure from spectral-element waveform tomography. *Geophys. J. Int.*, 2014, **199**(3), 1303–1327.
96. Levandowski, W., Boyd, O. S. and Ramirez-Guzmán, L., Dense lower crust elevates long-term earthquake rates in the New Madrid seismic zone. *Geophys. Res. Lett.*, 2016, **43**(16), 8499–8510.
97. Wolin, E., Stein, S., Pazzaglia, F., Meltzer, A., Kafka, A. and Berti, C., Mineral, Virginia, earthquake illustrates seismicity of a passive aggressive margin. *Geophys. Res. Lett.*, 2012, **39**(2), L02305; doi:10.1029/2011GL050310.
98. Becker, T. W., Lowry, A. R., Faccenna, C., Schmandt, B., Borsa, A. and Yu, C., Western US intermountain seismicity caused by changes in upper mantle flow. *Nature*, 2015, **524**(7566), 458–461.
99. Anderson, D. L., The thermal state of the upper mantle; no role for mantle plumes. *Geophys. Res. Lett.*, 2000, **27**(22), 3623–3626.
100. Anderson, D., The persistent mantle plume myth. *Aust. J. Earth Sci.*, 2013, **60**(6–7), 657–673.
101. Burke, K., Steinberger, B., Torsvik, T. H. and Smethurst, M. A., Plume generation zones at the margins of large low shear velocity provinces on the core–mantle boundary. *Earth Planet. Sci. Lett.*, 2008, **265**(1), 49–60.
102. Thorne, M. S., Garnero, E. J. and Grand, S. P., Geographic correlation between hot spots and deep mantle lateral shear-wave velocity gradients. *Phys. Earth Plan. Inter.*, 2004, **146**(1), 47–63.
103. Steinberger, B. and Torsvik, T. H., A geodynamic model of plumes from the margins of large low shear velocity provinces. *Geochem., Geophys., Geosyst.*, 2012, **13**(1), Q01W09; doi:10.1029/2011GC003808.
104. McNamara, A. K. and Zhong, S., Thermochemical structures beneath Africa and the Pacific Ocean. *Nature*, 2005, **437**(7062), 1136–1139.
105. Garnero, E. J., McNamara, A. K. and Shim, S.-H., Continent-sized anomalous zones with low seismic velocity at the base of earth's mantle. *Nature Geosci.*, 2016, 481–489.
106. Dziewonski, A. M., Mapping the lower mantle: determination of lateral heterogeneity in *P* velocity up to degree and order 6. *J. Geophys. Res. B*, 1984, **89**(7), 5929–5952.
107. Becker, T. W. and Boschi, L., A comparison of tomographic and geodynamic mantle models. *Geochem., Geophys., Geosyst.*, 2002, **3**, 1003; doi:10.1029/2001GC000168.

108. Simmons, N. A., Forte, A. M. and Grand, S. P., Joint seismic, geodynamic and mineral physical constraints on three-dimensional mantle heterogeneity: implications for the relative importance of thermal versus compositional heterogeneity. *Geophys. J. Int.*, 2009, **177**(3), 1284–1304.
109. Garnero, E. J., Lay, T. and McNamara, A., Implications of lower-mantle structural heterogeneity for the existence and nature of whole-mantle plumes. *Geol. Soc. Am. Spec. Pap.*, 2007, **430**, 79–101.
110. Nakagawa, T. and Tackley, P. J., Effects of low-viscosity post-perovskite on thermo-chemical mantle convection in a 3-D spherical shell. *Geophys. Res. Lett.*, 2011, **38**, L04309; doi: 10.1029/2010GL046494.
111. Lay, T., Hernlund, J., Garnero, E. J. and Thorne, M. S., A post-perovskite lens and *D*″ heat flux beneath the central Pacific. *Science*, 2006, **314**(5803), 1272–1276.
112. Cobden, L., Thomas, C. and Trampert, J., Seismic detection of post-perovskite inside the earth. In *The Earth's Heterogeneous Mantle*, Springer International Publishing, 2015, pp. 391–440.
113. Kuo, C. and Romanowicz, B., On the resolution of density anomalies in the earth's mantle using spectral fitting of normal-mode data. *Geophys. J. Int.*, 2002, **150**(1), 162–179.
114. Koelemeijer, P., Deuss, A., Ritsema, J. and van Heijst, H., Normal mode insights into the long wavelength velocity and density structure of the lowermost mantle. In AGU Fall Meeting Abs., 2014, vol. 1.
115. Nakagawa, T., Tackley, P. J., Deschamps, F. and Connolly, J. A., Incorporating self-consistently calculated mineral physics into thermochemical mantle convection simulations in a 3-D spherical shell and its influence on seismic anomalies in earth's mantle. *Geochem., Geophys., Geosyst.*, 2009, **10**, Q03004; doi:10.1029/2008GC002280.
116. Mulyukova, E., Steinberger, B., Dabrowski, M. and Sobolev, S. V., Survival of LLSVPs for billions of years in a vigorously convecting mantle: replenishment and destruction of chemical anomaly. *J. Geophys. Res. B*, 2015, **120**(5), 3824–3847.
117. Tolstikhin, I., Kramers, J. and Hofmann, A., A chemical earth model with whole mantle convection: the importance of a core–mantle boundary layer (*D*?) and its early formation. *Chem. Geol.*, 2006, **226**(3), 79–99.
118. Labrosse, S., Hernlund, J. and Coltice, N., A crystallizing dense magma ocean at the base of the earth's mantle. *Nature*, 2007, **450**(7171), 866–869.
119. Lee, C. T. A., Luffi, P., Höink, T., Li, J., Dasgupta, R. and Hernlund, J., Upside-down differentiation and generation of a primordial lower mantle. *Nature*, 2010, **463**(7283), 930–933.
120. Torsvik, T. H., Burke, K., Steinberger, B., Webb, S. J. and Ashwal, L. D., Diamonds sampled by plumes from the core–mantle boundary. *Nature*, 2010, **466**(7304), 352–355.
121. Garnero, E. J. and McNamara, A. K., Structure and dynamics of earth's lower mantle. *Science*, 2008, **320**(5876), 626–628.
122. Manglik, A. and Christensen, U., Effect of lithospheric root on decompression melting in plume–lithosphere interaction models. *Geophys. J. Int.*, 2006, **164**(1), 259–270.
123. Ishii, M. and Tromp, J., Normal-mode and free-air gravity constraints on lateral variations in velocity and density of earth's mantle. *Science*, 1999, **285**(5431), 1231–1236.
124. Su, W. J. and Dziewonski, A. M., Simultaneous inversion for 3-D variations in shear and bulk velocity in the mantle. *Phys. Earth Planet. Inter.*, 1997, **100**(1), 135–156.
125. Van der Hilst, R., Widiyantoro, S. and Engdahl, E., Evidence for deep mantle circulation from global tomography. *Nature*, 1997, **386**, 578–584.
126. Cammarano, F., Goes, S., Vacher, P. and Giardini, D., Inferring upper-mantle temperatures from seismic velocities. *Phys. Earth Planet. Inter.*, 2003, **138**(3), 197–222.
127. Karato, S. I. and Karki, B. B., Origin of lateral variation of seismic wave velocities and density in the deep mantle. *J. Geophys. Res. B*, 2001, **106**(10), 21771–21783.
128. Jordan, T., Continents as a chemical boundary layer. *Philos. Trans. R. Soc. London, Ser. A*, 1981, **301**(1461), 359–373.
129. Robertson, G. and Woodhouse, J., Ratio of relative S to P velocity heterogeneity in the lower mantle. *J. Geophys. Res. B*, 1996, **101**(9), 20041–20052.
130. Masters, G., Laske, G., Bolton, H. and Dziewonski, A., The relative behavior of shear velocity, bulk sound speed, and compressional velocity in the mantle: implications for chemical and thermal structure. Earth's deep interior: mineral physics and tomography from the atomic to the global scale. *Earth's Deep Interior*, 2000, 63–87.
131. Trampert, J., Deschamps, F., Resovsky, J. and Yuen, D., Probabilistic tomography maps chemical heterogeneities throughout the lower mantle. *Science*, 2004, **306**(5697), 853–856.
132. van der Hilst, R. D. and Kárason, H., Compositional heterogeneity in the bottom 1000 kilometers of Earth's mantle: toward a hybrid convection model. *Science*, 1999, **283**(5409), 1885–1888.
133. Ishii, M. and Tromp, J., Constraining large-scale mantle heterogeneity using mantle and inner-core sensitive normal modes. *Phys. Earth Planet. Inter.*, 2004, **146**(1), 113–124.
134. Hager, B. H., Mantle viscosity: a comparison of models from postglacial rebound and from the geoid, plate driving forces, and advected heat flux. In *Glacial Isostasy, Sea-level and Mantle Rheology*, Springer, 1991, pp. 493–513.
135. Mitrovica, J. and Forte, A., New insights obtained from joint inversions for the radial profile of mantle viscosity. *Phys. Chem. Earth*, 1998, **23**(9), 857–863.
136. Mitrovica, J. and Forte, A., A new inference of mantle viscosity based upon joint inversion of convection and glacial isostatic adjustment data. *Earth Planet. Sci. Lett.*, 2004, **225**(1), 177–189.
137. Pavlis, N. K., Holmes, S. A., Kenyon, S. C. and Factor, J. K., An earth gravitational model to degree 2160: EGM2008. EGU General Assembly, 2008, pp. 13–18.
138. Laske, G., Masters, G., Ma, Z. and Pasyanos, M., CRUST1.0: an updated global model of Earth's crust. *Geophys. Res. Abs.*, 2012, **14**.
139. Amante, C. and Eakins, B. W., ETOPO1 1 arc-minute global relief model: procedures, data sources and analysis. National Geophysical Data Center, NESDIS, NOAA, US Dept Commerce, Boulder, CO, USA, 2009.
140. Conrad, C. P. and Lithgow-Bertelloni, C., Influence of continental roots and asthenosphere on plate-mantle coupling. *Geophys. Res. Lett.*, 2006, **33**, L05312; doi:10.1029/2005GL025621.

ACKNOWLEDGEMENTS. S.A. was supported by MoES grant MESO006. Maps were prepared using Generic mapping tools version 4.5.13. We thank students G. Thyagarajulu and J. Paul for their assistance. Comments from an anonymous reviewer helped improve the article.

doi: 10.18520/cs/v112/i07/1463-1473